Research Square

Preprints are preliminary reports that have not undergone peer review.
They should not be considered conclusive, used to inform clinical practice,
or referenced by the media as validated information.

Resurrected ancestral influenza A viruses recapitulate the avian-to-mammalian adaptation of European avian-like swine influenza virus

Wen Su
School of Public Health, Li Ka Shing Faculty of Medicine, The University of Hong Kong
Rhodri Harfoot
Department of Infectious Diseases, St. Jude Children's Research Hospital, Memphis, TN, USA
Yvonne Su
Duke-NUS Medical School https://orcid.org/0000-0003-4349-9211
Jennifer DeBeauchamp
Department of Infectious Diseases, St. Jude Children's Research Hospital
Udayan Joseph
Programme in Emerging Infectious Diseases, Duke-NUS Medical School
Jayanthi Jayakumar
Programme in Emerging Infectious Diseases, Duke-NUS Medical School
Jeri-Carol Crumpton
Department of Infectious Diseases, St. Jude Children's Research Hospital
Trushar Jeevan
Department of Infectious Diseases, St. Jude Children's Research Hospital
Adam Rubrum
Department of Infectious Diseases, St. Jude Children's Research Hospital
John Franks
Department of Infectious Diseases, St. Jude Children's Research Hospital
Philippe Pascua
Department of Infectious Diseases, St. Jude Children's Research Hospital
Christina Kackos
Department of Infectious Diseases, St. Jude Children's Research Hospital
Yuqin Zhang
School of Public Health, Li Ka Shing Faculty of Medicine, The University of Hong Kong
Mengting Zhang
School of Public Health, Li Ka Shing Faculty of Medicine, The University of Hong Kong
Yue Ji
School of Public Health, Li Ka Shing Faculty of Medicine, The University of Hong Kong
Christine H. T. Bui

The University of Hong Kong
Jeremy Jones
St. Jude Children's Research Hospital https://orcid.org/0000-0002-9980-2112
Lisa Kercher
Department of Infectious Diseases, St. Jude Children's Research Hospital
Scott Krauss
Department of Infectious Diseases, St. Jude Children's Research Hospital
Stephan Pleschka
University of Giessen
Michael CW Chan
The University of Hong Kong
Robert Webster
St. Jude Children's Research Hospital
Chung-Yi Wu
Genomics Research Center, Academia Sinica
Kristien Van Reeth
Gent University
Malik Peiris
University of Hong Kong https://orcid.org/0000-0001-8217-5995
Richard Webby
St. Jude Children's Research Hospital
Gavin Smith
Duke-NUS Medical School https://orcid.org/0000-0001-5031-468X
Hui-Ling Yen (hyen@hku.hk)
University of Hong Kong https://orcid.org/0000-0003-2493-3609

Article

Keywords: influenza virsu, avian-like swine influenza virus, avian-to-mammalian adaptation, guide pandemic preparedness resources, adapting viruses

Posted Date: April 30th, 2021

DOI: https://doi.org/10.21203/rs.3.rs-436907/v1

License: This work is licensed under a Creative Commons Attribution 4.0 International License.
Read Full License

Version of Record: A version of this preprint was published at Nature Microbiology on October 26th, 2021. See the published version at https://doi.org/10.1038/s41564-021-00976-y.

Abstract

The emergence of a pandemic influenza virus may be better anticipated if we better understand the evolutionary steps taken by avian influenza viruses as they adapt to mammals. We used ancestral sequence reconstruction to resurrect viruses representing initial adaptive stages of the European avian-like H1N1 virus as it transitioned from avian to swine hosts. We demonstrate that efficient transmissibility in pigs was gained through stepwise adaptation after 1983. These time-dependent adaptations resulted in changes in hemagglutinin receptor binding specificity and increased viral polymerase activity. An NP-R351K mutation under strong positive selection increased the transmissibility of a reconstructed virus. The stepwise-adaptation of a wholly avian influenza virus to a mammalian host suggests a window where targeted intervention may have highest impact. Successful intervention will, however, require strategic coordination of surveillance and risk assessment activities to identify these adapting viruses and guide pandemic preparedness resources.

Introduction

Pandemic influenza viruses must acquire an ability for sustained human-to-human transmissibility, an ability aided by antigenic novelty and a resulting absence of human population immunity. While antigenic novelty can be readily expected for influenza viruses emerging from animal reservoirs, sustained transmissibility is a rare trait that needs to be acquired to foster optimal interactions with the complex cellular receptors, replicative machinery and innate immune responses of the new host. How influenza viruses acquire these traits is poorly defined[1-5]. The emergence of the A(H1N1)pdm09 pandemic influenza virus from pigs is a clear reminder of the feasibility of influenza viruses to cross mammalian species barriers and become established in humans[6]. However, thousands of human zoonotic infections caused by avian influenza viruses of H9N2, H5N1, H7N9 or H5N6 subtypes have been detected, but fortuitously, none of these avian-origin viruses have yet acquired the ability for sustained human-to-human transmissibility[7]. In addition to the A(H1N1)pdm09 virus, only a limited number of avian-origin influenza viruses are known to have successfully crossed the species barriers and established in a new mammalian host. These viruses offer the best opportunities to identify the molecular determinants for successful establishment of avian influenza viruses in mammals.

The European avian-like (EA) swine H1N1 lineage viruses transitioned from avian to swine hosts in the late 1970s[8,9], with all eight gene segments derived from Eurasian avian influenza viruses[10,11]. Since then, these viruses have substantially impacted animal and human health. They are now prevalent among pigs in China and in European countries[9,12-14], they donated the NA and M gene segments to the A(H1N1)pdm09 virus[6], and they have demonstrated pandemic potential, including resistance to human MxA[14,15], airborne transmissibility in ferrets[13,16], and antigenic novelty (eg. limited cross-reactivity with the antibodies that human population has developed against circulating influenza strains)[13,14,16]. Here, we identify and characterize the time-dependent molecular changes that were responsible for the full adaptation of the EA swine virus since the avian-to-swine interspecies jump. By resurrecting

computationally predicted ancestral viruses at different points in the early evolution of EA swine viruses[17,18], we specifically investigated if the sustained swine transmissibility of EA swine viruses was an intrinsic trait of the precursor avian influenza virus or if it was acquired in pigs through subsequent adaptations.

Results

EA swine H1N1 viruses demonstrated stepwise changes in receptor-binding properties. Since a change in receptor binding specificity is a critical step for avian-to-mammalian interspecies transmission[19], we initially examined the receptor binding preference of eleven representative EA swine viruses isolated from 1979 to 2011 (Supplementary Fig. 1). Compared to the avian H1N1 influenza virus A/duck/Bavaria/2/1977 (DK/77), which preferentially recognizes α-2,3 sialosides (Fig. 1a), early EA swine viruses represented by A/swine/Germany/2/1981 (SW/81), showed dual binding specificity to both α-2,3 and α-2,6 sialosides (Fig. 1b). The EA swine viruses isolated after 1990, represented by A/swine/Schleswig-Holstein/1/1992 (SW/92), bound exclusively to α-2,6-linked sialosides (Fig. 1c). In agreement with previous results[20,21], the EA swine viruses showed no apparent time-dependent changes in their hemagglutinin fusion pH with values ranging from pH 5.2 to 5.8 (Supplementary Table 1).

The replication efficiency of avian (DK/77) and swine (SW/81 and SW/92) influenza viruses exhibiting differential binding for α-2,3 and α-2,6 sialosides (Fig. 1a,b,c) were further evaluated *in vitro*. In new-born pig trachea (NPTr) cells, SW/81 replicated to higher titers than DK/77 and SW/92 viruses at all time points (Two-way ANOVA and Tukey's multiple comparisons post hoc test, $P < 0.01$)(Fig. 1d). In pig lung explants, SW/81 and SW/92 replicated to higher titers than DK/77 at 24 hours post-infection (hpi) (Two-way ANOVA, $P < 0.01$ and Tukey's multiple comparisons post hoc test, $P < 0.05$) (Fig. 1e). No significant differences in replication were observed in the pig trachea explants (Fig. 1f). Taken together, these results show that the EA swine viruses underwent progressive adaptations and acquired the exclusive binding specificity for α-2,6 sialosides (Supplementary Fig. 1). Despite of increased binding specificity for α-2,6 sialosides, swine viruses SW/81 and SW/92 showed marginally enhanced replication over the avian virus DK/77 in the lung explants but not in the pig trachea cell line or explants.

EA swine H1N1 viruses demonstrated stepwise changes in contact transmission potential in pigs. The contact transmission potential of DK/77, SW/81, and SW/92 viruses were further compared in 3-4 weeks old piglets. Donor pigs were intranasally inoculated with 10^6 plaque forming units (pfu) of the virus and were co-housed with naïve contact pigs on 1 day post-inoculation (dpi) at a 2:2 donor-contact ratio. Each experiment was independently performed in duplicate with a total of 4 donors and 4 direct contacts. Area under the curve (AUC) were calculated to approximate total viral load over the course of infection (Fig. 1g, h, i). In inoculated donors, the avian DK/77 virus replicated (mean ± SD AUC = 1.58 ± 1.59) to lower titers than the swine viruses SW/81 (mean ± SD AUC = 3.81 ± 1.1) and SW/92 (mean ± SD AUC = 5.8 ± 0.78), respectively (Kruskal–Wallis test, $P = 0.0031$, Dunn's post hoc test at $P = 0.61$ and 0.013, respectively). There was no significant difference in AUC between SW/81 and SW/92 inoculated donors (Dunn's post hoc test, $P = 0.35$). Correspondingly, the avian DK/77 virus failed to transmit to any contact (Fig. 1g), and

none of the donor or the contact pigs seroconverted [hemagglutination inhibition (HI) titer < 1:20]. SW/81 virus replicated better than the DK/77 virus with infectious virus detected in the nasal cavity of 4/4 donors and seroconversion in 3/4 donors (HI titers at 1:40 to 1:80). However, SW/81 transmitted inefficiently to contact pigs as infectious virus was detected transiently in 2/4 contacts at later time points post-exposure (Fig. 1h), with seroconversion detected in 2/4 contacts (1:40). In contrast, robust replication and transmission of SW/92 virus was detected in 4/4 donors and 4/4 contacts (Fig. 1i), with seroconversion detected in all donor (1:160 to 1:320) and contact pigs (1:80 to 1:320). These results suggest that the EA swine viruses may have gone through sequential adaptation during the avian-to-pig host transition by increasing replicative capacity in pig nasal tissues followed by developing efficient transmissibility among pigs.

Resurrected ancestral EA swine H1N1 viruses possessed comparable phenotypes as the wild-type viruses. To comprehensively map the molecular changes associated with EA swine H1N1 virus adaptation in pigs, maximum likelihood phylogenies for the eight viral gene segments were constructed using EA swine viruses isolated from 1979 to 2014 and avian viruses isolated from 1949 to 2013 (Supplementary Fig. 2). Ancestral sequence reconstruction was used to infer ancestral sequences of four major nodes that represent different evolutionary stages of EA swine influenza viruses (Fig. 2a). Four EA resurrected viruses were generated using gene synthesis and plasmid-based reverse genetics. Their full genomes were deposited to the public database GISAID (accession numbers: EPI_ISL_539852-5). The recombinant. RG-EA1, representing the precursor virus of EA swine viruses, was constructed based on the inferred nodal sequences at the split between avian and EA swine lineages (Fig. 2a; Node 1 in Supplementary Fig. 2). RG-EA2 virus was constructed to represent the early evolutionary stage of EA swine viruses in 1979-1983 (Fig. 2a; Node 2 in Supplementary Fig. 2), while RG-EA3 and RG-EA4 viruses represented EA swine viruses in 1984-1987 and 1988-1992, respectively (Fig. 2a; Nodes 3 and 4 in Supplementary Fig. 2).

The receptor binding profiles of the reconstructed RG-EA1, EA2, EA3, EA4 viruses were compared. The avian-like precursor RG-EA1 virus showed exclusive binding to α-2,3 sialosides (Fig. 2b). The RG-EA2 virus showed dual binding for α-2,3 and α-2,6-linked sialosides (Fig. 2c) that resembled early EA swine isolates (Fig. 1b and Supplementary Fig. 1). The RG-EA3 and EA4 viruses bound predominantly to α-2,6-linked sialosides (Fig. 2d, e) and resembled late EA swine isolates (Fig.1c and Supplementary Fig. 1). The four resurrected EA viruses showed comparable HA stability with fusion pH 5.8-5.9 (Supplementary Table 2) that more resembled EA swine viruses but not the avian virus DK/77 (Supplementary Table 1). In NPTr cells, RG-EA1 replicated to significantly lower titers than RG-EA2, EA3, EA4 viruses at 12, 24 and 36 hpi (Two-way ANOVA, $P < 0.01$ and Tukey's multiple comparisons post hoc test, $P < 0.05$; Fig. 2f). We also observed a time-dependent increase in the polymerase activity from RG-EA1 to RG-EA4 in NPTr cells (Fig. 2g), with RG-EA4 showing the highest polymerase activity in human 293T cells using the minigenome assay (Fig. 2h)[22,23]. These results also support the time-dependent adaptation of EA swine viruses in pigs since its introduction from the avian hosts.

EA swine H1N1 viruses sequentially acquired efficient pig-to-pig transmissibility after 1983. RG-EA1, EA2, EA3, and EA4 viruses were further evaluated for their transmissibility among pigs by direct contact. The avian-like RG-EA1 virus was transiently detected in the nasal swabs of 3/4 donors and 1/4 contacts (Fig. 3a), with none of the donors or contacts seroconverted. RG-EA2, which genetically resembles 1979-1983 era EA swine influenza viruses was transiently detected in 2/4 donors and 1/4 contacts (Fig. 3b), with 1/4 donors seroconverted (1:40). RG-EA3 and EA4, which resemble post 1983 era EA swine influenza viruses replicated more efficiently in all donors (Fig. 3c,d) and were transmitted to 4/4 contacts with seroconversion detected in all donors (1:40 to 1:320) and contacts (1:320 to 1:640). Viral loads detected in the nasal swabs of donors inoculated with RG-EA1 (mean ± SD AUC = 2.48 ± 2.25), EA2 (mean ± SD AUC = 0.91 ± 1.05), EA3 (mean ± SD AUC = 4.72 ± 3.23), or EA4 (mean ± SD AUC = 5.18 ± 1.39) were moderately different (Kruskal–Wallis test, $P = 0.051$). Collectively, we noted a positive correlation between viral loads detected in donor nasal swabs and viral transmissibility in pigs (Spearman's r = 0.90, $p = 0.014$) (Fig. 3e), suggesting the importance of achieving high viral loads at the nasal epithelial cells prior to acquiring efficient transmissibility.

Introducing HA and NA genes derived from RG-EA3 virus did not increase transmissibility of RG-EA2 virus in pigs. Thirty-three amino acid differences exist between the non-transmissible RG-EA2 and transmissible EA3 viruses with changes in the PB2(N = 5), PB1(N = 3), PA(N = 2), HA1(N = 9), HA2(N = 3), NP(N = 4), NA(N = 1), and NS1(N = 6) proteins (Fig. 4a). Among the amino acid differences found in the HA protein of RG-EA2 and EA3 viruses, HA1-N121T, HA1-Y138H, HA1-N207Y, HA1-K311Q, HA2-A65S, and HA2-D158N (H1 numbering) were detected at high frequency (>90%) among EA swine viruses isolated from 1979-2016 (Fig. 4a). Introducing these mutations into the HA protein of RG-EA2 virus significantly reduced binding for α-2,3-linked sialosides and marginally enhanced binding for α-2,6-linked sialosides (Fig. 4b). In the NA protein, RG-EA2 and RG-EA3 differed by the Y344N mutation (N1 numbering) (Fig. 4a). RG-EA1, EA3 and EA4 showed comparable *K*m that are higher than that of RG-EA2 (One-way ANOVA and Turkey's multiple comparisons post hoc test, $P = 0.15$); however, the avian-like RG-EA1 showed the highest V_{max} ($P < 0.01$) (Supplementary Table 2).

To investigate if the surface gene segments from RG-EA3 dictate the different transmission phenotypes between RG-EA2 and RG-EA3 viruses, we constructed RG-EA2xEA3^{SG} virus that contained the internal genes from RG-EA2 and the surface genes derived from RG-EA3. RG-EA2xEA3^{SG} virus was transiently detected in the nasal swabs of 2/4 inoculated donors with peak titers detected on 8 and 10 dpi (Fig. 4c), respectively; none of the donors seroconverted by 11 dpi. RG-EA2xEA3^{SG} was transiently detected in 2/4 contacts with peak titers at late time points on 11 and 13 dpe, respectively (Fig. 4c), with none of the contact pigs seroconverted. These results suggest that introducing the HA and NA genes of RG-EA3 virus was not sufficient to confer increase transmissibility for RG-EA2 virus.

Molecular determinants associated with efficient transmission in pigs reside in the internal genes. Among 20 amino acids that differentiate the internal proteins of RG-EA2 and -EA3 viruses, PB1-Q621R and NP-R351K were under positive selection and were detected at high frequencies (> 90%) among EA swine influenza viruses isolated from 1979 to 2018 (Fig. 4a). PB1-R621 and NP-K351 were also highly enriched

among classical H1N1 swine viruses and human influenza A viruses isolated from 1933 to 2019 (Fig. 5a). Introduction of the PB1-Q621R but not the NP-R351K mutation increased the polymerase activity of RG-EA2 (One-way ANOVA and Tukey's multiple comparisons post hoc test, $P < 0.01$; Fig. 5b). Both PB1-R621Q and NP-K351R mutations reduced the polymerase activity of RG-EA3 ($P < 0.01$; Fig. 5b). In NPTr cells, RG-EA2 $^{PB1\text{-}Q621R,NP\text{-}R351K}$ replicated to higher titers than RG-EA2 and RG-EA2 $^{NP\text{-}R351K}$ viruses at 24 hpi ($P = 0.019$) and 36 hpi ($P = 0.024$), respectively (Fig. 5c). Interestingly, the NP-R351K mutation facilitated accumulation of viral RNP in the nucleus at earlier time points when compared to RG-EA2 virus ($P < 0.05$; Fig. 5d,e).

Next, we constructed RG-EA2xEA3^{IG} virus contained surface genes from RG-EA2 and internal genes from RG-EA3. In inoculated donors, RG-EA2xEA3^{IG} virus was detected in the nasal swabs of 2/4 inoculated donors, with peak titers detected earlier on 4 and 6 dpi (Fig. 5f) than those inoculated with the RG-EA2xEA3^{SG} virus (Fig. 4c). In contact pigs, RG-EA2xEA3^{IG} virus was transiently detected in 2/4 contacts (Fig. 5f), with peak titers detected earlier on 7 dpc (Fig. 5f) than those exposed to RG-EA2xEA3^{IG} on 11 and 13 dpc (Fig. 4c); seroconversion was detected in one pig (1:160). These results suggest that RG-EA2xEA3^{IG} virus showed better replication in inoculated donors and transmitted more rapidly to contact pigs than the RG-EA2xEA3^{SG} virus. However, the inefficient transmissibility of the RG-EA2xEA3^{IG} virus may be due to the presence of deleterious mutations in the exchanged gene segments that counteracted the effects of mutations that facilitated transmission.

Since NP-R351K and PB1-Q621R mutations were under positive selection, we focused on these two mutations and compared the transmissibility of RG-EA2$^{NP\text{-}R351K}$ and RG-EA2$^{PB1\text{-}Q621R,\ NP\text{-}R351K}$ viruses in pigs. RG-EA2$^{NP\text{-}R351K}$ was detected from the nasal swabs of 4/4 donors and 4/4 contacts (Fig. 5g), and seroconversion was detected in 4/4 donors (1:80 to 1:160) and 3/4 contacts (1:80 to 1:160). RG-EA2$^{PB1\text{-}Q621R,NP\text{-}R351K}$ was detected from the nasal swabs of 4/4 donors and 4/4 contacts (Fig. 5h), and all donors (1:80 to 1:160) and contacts (1:160 to 1:640) seroconverted. The total amount of virus shed by the RG-EA2$^{NP\text{-}R351K}$ inoculated donors (mean ± SD AUC = 2.74 ± 2.63) was comparable to that of the RG-EA2$^{PB1\text{-}Q621R,NP\text{-}R351K}$ inoculated donors (mean ± SD AUC = 3.78 ± 1.67; two-sided Mann-Whitney test, $P = 0.69$). Notably, one donor pig infected with RG-EA2$^{PB1\text{-}Q621R,NP\text{-}R351K}$ shed high viral titers in the nasal swabs and was euthanized on days 4 post-infection due to respiratory distress with abdominal distention, severe lethargy, and vomiting (Fig. 5h). In contact pigs, viral load shed by RG-EA2$^{NP\text{-}R351K}$ infected contacts (mean ± SD AUC = 3.04 ± 1.57) was slightly lower than that of the RG-EA2$^{PB1\text{-}Q621R,NP\text{-}R351K}$ infected contacts (mean ± SD AUC = 5.4 ± 1.31; two-sided Mann-Whitney test, $P = 0.11$). Next-generation sequencing analyses were performed on the peak-titer nasal swab samples of each contact pig infected with RG-EA2$^{NP\text{-}R351K}$ or RG-EA2$^{PB1\text{-}Q621R,NP\text{-}R351K}$ and we did not observe common adaptive mutations in more than 1 pig (Supplementary Table 3). Taken together, these results showed that introducing the NP-R351K mutation was sufficient to enhance the transmissibility of the reconstructed early EA2 swine virus with a PB1-Q621R mutation increasing replication.

Sequence analyses of archived EA swine viruses in pig lung homogenates from 1979 validated the ancestral sequence reconstruction approach. An inherent difficulty in following the evolutionary steps of influenza virus host range transitions is the lack of many viral isolates representing ancestral and intermediate states. We adopted an evolution-guided approach to reconstruct recombinant EA swine viruses based on the posterior distributions of ancestral states at their corresponding nodes of the virus phylogeny. This approach may be biased if the viral sequences contained mutations that emerge after sequential passages in embryonated chicken eggs or in cell culture. To validate the predicted ancestral sequences we reconstructed, direct sequencing of EA swine viruses in two archived pig lung homogenates from 1979 was performed: a partial genome of A/swine/Belgium/1/1979 (designated as Be01-lung; GISAID accession numbers: EPI_ISL_1055769) and full genome of A/swine/Belgium/2/1979 (designated as Be02-lung; GISAID accession numbers: EPI_ISL_1055773) were recovered. The Be01-lung and Be02-lung sequences shared 98.8–99.3% nucleotide homology and 98.9–99.4% amino acid homology with the RG-EA2 virus. Among 33 different amino acids between RG-EA2 and RG-EA3 viruses, the full genome of Be02-lung only differed from the RG-EA2 virus by a single amino acid residue (PB2-483M in Be02-lung and T in RG-EA2) (Fig. 6). In comparison with RG-EA2, the partial sequence of Be01-lung showed four amino acid differences at HA1 residues that are highly variable among EA swine influenza viruses (Fig. 6). Importantly, the PB1-621 and NP-351 residues of the two pig lung homogenates were identical to that of the RG-EA2 virus (Fig. 6). Collectively, both original viral sequences shared high homology with the reconstructed ancestral sequence of RG-EA2 that genetically resembles 1979-1983 era EA swine influenza viruses. Additional serial passages of recombinant RG-EA2 virus carrying the HA and NA genes derived from Be02-lung (designated as RG-Be02-lung^{SG}xEA2^{IG}) or RG-EA1, RG-EA2, RG-EA3, RG-EA4 viruses in embryonated chicken eggs, MDCK cells, or NPTr cells failed to identify any common amino acid changes associated with egg adaptation (Supplementary Table 4-6).

Discussion

Understanding the molecular mechanisms that facilitate efficient adaptation and transmission within a new host following inter-species transmission events is essential for future pandemic preparedness. Using the ancestral sequence reconstruction approach, we demonstrated that sustained pig-to-pig transmissibility of the EA swine influenza viruses was not an intrinsic property possessed by the avian-like precursor virus prior to its introduction into mammals. Instead, EA swine influenza viruses acquired efficient transmissibility after 1983 through stepwise avian-to-pig adaptations. Inefficient transmission was observed for the EA swine viruses between 1979 and 1983 (SW/81 virus), suggesting that transmission in pigs was maintained at low levels during this period while the virus adapted to its new host. Specifically, we observed time-dependent changes in receptor binding specificity from recognizing both α-2,3 and α-2,6-linked sialosides (RG-EA2) to recognizing only α-2,6-linked sialosides (RG-EA3 and RG-EA4) and gradually increased polymerase activity, which likely contributed to viral replication in pig nasal epithelial cells and the subsequent efficient transmissibility in pigs. Interestingly, further analyses using RG-EA2 and RG-EA3 viruses that differed in the receptor binding specificity and transmission potential in pigs, identified that the NP-R351K mutation was the minimal molecular change required to

significantly enhance transmissibility in pigs. Our results illustrated the multi-step process for avian influenza viruses to sequentially adapt in mammalian hosts.

Ancestral sequence reconstruction is a powerful tool that has been used to investigate the function of "extinct" genes[24]. We and others showed that reconstructed ancestral H5 proteins may induce cross-reactive antibodies against various sub-clades of H5 avian influenza viruses[18,25]. Here, we show that ancestral sequence reconstruction is an excellent approach to study important adaptive processes underpinning the interspecies transmission of influenza viruses. Although the predictive power of corresponding algorithms is dependent on the number of available sequences, direct sequencing of EA swine influenza viruses from archived pig lung homogenates in 1979 has confirmed the robustness of the approach in constructing representative sequences at different evolutionary nodes.

Our results show that the adaptation of EA viruses to the swine host was progressive. Avian and human influenza viruses specifically bind to α2,3-linked and α2,6-linked sialosides, respectively[20,26]. In the transition from the avian host to the swine host, early EA swine viruses (represented by RG-EA2 virus) acquired binding for α-2,6-linked sialosides and retained binding for α2,3-linked sialosides, and later EA swine viruses (represented by RG-EA3 and RG-EA4 viruses) have lost binding for α-2,3-linked sialosides and exhibited exclusive binding to α-2,6-linked sialosides. Our results are consistent with a previous study that reported reduced affinity for 3'LN-PAA of the early EA swine viruses[27]. Early EA swine influenza viruses were cultured in chicken embryonated eggs, which may select or maintain HA mutations that enabled binding for α-2,3-linked sialosides. The fact that a single NP-R351K mutation was able to facilitate efficient transmission of the RG-EA2 virus that possessed dual binding specificity indicates that an exclusive α-2,6 binding specificity may not be essential for swine influenza viruses to transmit efficiently in pigs.

The NP-R351K amino acid change has been under strong positive selection not only among the EA swine viruses but also in other human and swine influenza viruses. The NP gene of human seasonal A(H1N1), A(H2N2), and A(H3N2) influenza viruses has descended from the 1918 pandemic influenza virus[28.] The 1918 NP protein differed by the avian consensus sequence by 6 amino acids and was likely derived from the avian host prior to 1918 through genetic reassortment[29]. The 1918 virus contained NP-R351, which is consistent to the putative avian origin. The NP-R351K mutation has been quickly fixed among the human seasonal A(H1N1) viruses from 1918 to 1957, with 39 out of 42 (92.86%) available sequences containing K351. This adaptive mutation has been maintained in human A(H2N2) and A(H3N2) viruses, as K351 is found in 100% (129/129) A(H2N2) sequences from 1957 to 1968, and in 99.93% (26,895/26,915) A(H3N2) sequences from 1968 to 2019. The recent A(H1N1)pdm09 virus derived its NP gene from the classical swine influenza viruses that share the same origin as the 1918 pandemic virus[6]. Since the NP-R351K mutation was also fixed in 97.08% (1,993/2,053) of the classical swine influenza viruses, the A(H1N1)pdm09 virus continues to harbour the NP-R351K mutation at a high frequency (99.97%, 17,621/17,626) from 2009 to 2019.

NP residue 351 is located in proximity to one of three nuclear localization signals in NP[30-32] and in proximity to residue 319 in the monomeric NP form[33]. Previous studies showed that NP-N319K mediated a switch from importin-α3 to importin-α7 dependency upon avian–to-mammalian adaptation[34], and 93.64% (368/393) of EA H1N1 swine viruses possess N at position 319. It is possible that NP-R351K change may facilitate nucleus importation of viral RNP, which is consistent to our observation. In addition, interaction with interferon-induced MxA protein may select NP residues that confer MxA resistance[35-37]. The potential interaction of the NP-R351K mutation with Mx1 and MxA has been studied in the context of A(H1N1)pdm09[36] and EA swine influenza viruses[15], highlighting that the NP-R351K mutation alone did not confer resistance to Mx1 or MxA. Further studies are needed to delineate the functional role conferred by the NP-R351K mutation.

Our results show that these resurrected ancestral influenza A viruses represent excellent models for the study of interspecies transmission and host adaptation. RNA viruses will continue to cross species barriers and there is a need to maintain vigilance for the next pandemic virus. Our results highlight the importance of continuous surveillance that should be strategically coordinated with risk assessment studies in order to identify viruses with pandemic potential before they become fully adapted in the mammalian species. Intervention strategies implemented prior to full adaption to the new host are most likely to be successful and represent the best use of limited preparedness resources.

Methods

Cells and viruses. Madin-Darby Canine Kidney (MDCK) cells were obtained from the American Type Culture Collection (ATCC) and were maintained in minimal essential medium (MEM) supplemented with 10% fetal calf serum (FCS), 1% penicillin-streptomycin (P/S), and 1% vitamins, and buffered with 25 mM HEPES. Human embryonic kidney 293T (293T) cells were obtained from ATCC and were maintained in Opti-MEM supplemented with 5% FCS and 1% P/S. New-born pig trachea (NPTr) cells were obtained from Istituto Zooprofilattico Sperimentale, della Lombardia e dell'Emilia Romagna and were maintained in MEM supplemented with 10% FCS, 1% P/S, and 1% sodium pyruvate. African green monkey kidney (Vero) cells were obtained from ATCC and were maintained in MEM supplemented with 10% FCS and 1% P/S. Cells were cultured at 37^{o}C in 5% CO_2. All cells used in the study were routinely tested negative for *Mycoplasma sp.* using real-time PCR conducted by the Faculty Core Facility, the University of Hong Kong.

Avian influenza virus A/duck/Bavaria/2/1977 (H1N1) and Eurasian avian-like (EA) swine influenza A(H1N1) viruses A/swine/Netherlands/3/1980, A/swine/Germany/2/1981, A/swine/Netherlands/12/1985, A/swine/Italy/670/1987, and A/swine/Schleswig-Holstein/1/1992 were kindly provided by Dr. Robert Webster from St. Jude Children's Research Hospital, Memphis, TN USA. EA swine influenza viruses A/swine/Arnsberg/6554/1979 (H1N1) was kindly provided by Prof. Stephan Pleschka from Justus-Liebig-University Giessen, Germany. EA swine influenza viruses, A/swine/Hong Kong/8512/2001, A/swine/Hong Kong/72/2007, A/swine/Hong Kong/1559/2008, A/swine/Hong Kong/NS29/2009, and A/swine/Hong Kong/NS4848/2011 were isolated and stored at the University of

Hong Kong. Viruses were grown at a multiplicity of infection (MOI) of 0.005 on MDCK cells cultured in MEM supplemented with 0.3% bovine serum albumin (BSA, Sigma-Aldrich, Missouri, USA), 1% P/S, and 1% vitamin , 25 mM HEPES and 1μg/mL L-1-tosylamide-2-phenylmethyl chloromethyl ketone (TPCK)-treated trypsin (Sigma-Aldrich, Missouri, USA) (designated as infection medium). The viruses used in the study were passaged twice on MDCK cells and their genomes were confirmed by Sanger sequencing (CGS, The University of Hong Kong; Table S1). All stock viruses were aliquoted and stored at -80 ^{o}C. The titer of stock viruses was calculated in plaque forming units per milliliter (pfu/mL).

Ancestral sequence reconstruction. Over 2,000 nucleotide sequences of HA-H1NX (N = 410), NA-HXN1 (N = 443) and HXNX (for all the 6 internal genes: PB2 (N = 454), PB1 (N = 427), PA (N = 397), NP (N = 417), MP (N = 495) and NS (N = 400) were downloaded from NCBI database before the year 2014. Sequences less than 500 bp were removed from the datasets. Identical sequences and outliers were also removed from the datasets. For each gene segment, 10 independent runs of maximum likelihood analyses were performed using RAxML ver 8.0[38]. Ancestral nucleotide sequences were inferred at internal nodes using the phylogenetic trees and the baseml program as implemented in the Lazarus software[39]. For each gene segment, internal nodes were assigned to indicate the transmission events of EA swine influenza virus from avian to swine and to also represent different evolutionary stages of EA swine influenza viruses in pigs. Amino acid substitutions were mapped onto maximum likelihood phylogenies using the treesub programme[40].

Generation of ancestral recombinant viruses by reverse genetics. The nodal sequences derived from the phylogenetic analyses of eight gene segments of avian and EA swine influenza viruses were synthesized by GeneArt and Synbio Techonogies (Monmouth Junction, New Jersey, USA). The synthesized genes were cloned into pHW2000 vector by mega-primers PCR as described[41,42]. Recombinant viruses were generated by transfecting eight plasmids into 293T cells. Virus titers were determined in 6-well plates on MDCK cells by plaque assay. All rescued viruses were propagated twice on MDCK cells at a MOI of 0.005 to prepare virus stocks. The stock viruses were aliquoted and stored at -80 ^{o}C. Their genomes were confirmed via Sanger sequencing.

Solid-phase binding assay. Binding profile of influenza viruses for 3'SLN (Neu5Aca2-3Galb1-4GlcNAcb-PAA-biotin) and 6'SLN (Neu5Aca2-6Galb1-4GlcNAcb-PAA-biotin) (Lectinity Holding Inc., Moscow, Russia) were analysed on a modified solid-phase direct-binding assay inside the Biosafety Level 2 facilities as described previously[43]. Briefly, two-fold series dilution of 3'SLN and 6'SLN were incubated in the wells of 96-well Pierce Streptavidin High Binding Capacity Plates (Thermo Fisher Scientific Inc., Rockford, USA) overnight at 4 ℃. The final concentrations of glycans ranged from 5 μg/mL to 0.1 μg/mL. Hemagglutinination units (HAU) were determined by hemagglutinination assays with 0.5% Turkey red blood cells. To reach sufficient HAU, some viruses were concentrated by using Amicon Ultra-15 centrifugal Filter Units (100 kDa; Merck, Darmstadt, Germany). The plates were washed with ice-cold PBS containing 0.1% Tween 20 (PBST) and viruses (diluted with 1% BSA in PBS to 64 HAU in 50 μL) was directly and incubated overnight at 4 ℃. After incubation, the plates were washed with ice-cold PBST and

virus bound to 3'SLN and 6'SLN was detected using the rabbit polyclonal antibody raised against HA of A/duck/NZL/160/1976 (H1N3) (Sino Biological Inc., Beijing, China) and a polyclonal Goat Anti-Rabbit Immunoglobulins/HRP (Dako, Glostrup, Denmark). After incubation, the plates were washed with PBST and were incubated with 3,3',5,5'-tetramethylbenzidine (TMB) (eBioscience Inc., San Diego, USA) for 15 min. The reaction was stopped with 0.5 M H_2SO_4, and the absorbance was measured at 450 nm in a FLUOstar OPTIMA microplate reader (BMG Labtech, Ortenberg, Germany).

Glycan microarray. A synthesized glycan microarray comprised of 38 glycans of α2,3-linked sialosides (glycan 1-38), 3 glycans containing both α2,3 & α2,6-linked sialosides (glycan 39-41) and 32 glycans of α2,6-linked sialosides (glycan 42-73) (Supplementary Fig. 3) was utilized for virus binding study using viruses that were inactivated by 0.025% formaldehyde for 7 days at 4 ^{o}C. Glycan array slides were blocked by SuperBlock™ (PBS) Blocking Buffer (Pierce, Rockford, USA) for 1 hour at room temperature. To avoid the influence of neuraminidase (NA), NA inhibitor zanamivir was added to virus stocks at a final concentration of 10 μM. Formalin-inactivated viruses were diluted to 64 HAU per 50 μL and 100 μL of the inactivated viruses were added to the wells of the glycan array. The array slides were incubated at room temperature with slow shaking (13 rpm) for 1 hour. The bound viruses were detected using a HA2-targeting human monoclonal antibody (MED18852) followed by goat anti-human IgG (H+L) secondary antibody labelled with Alexa Fluor 647 (Invitrogen TM, Thermo Fisher, USA). The slides were scanned by InnoScan 710 AL Microarray Scanner (Innopsys, Chicago, USA) equipped with two laser sources, visible wavelength 635nm and 532nm. The data were analyzed in GenePix Pro 6.0 software (Molecular Devices, San Jose, USA).

Syncytium formation assay. The assay was performed as described previously[22]. Vero cells in 48-well plates were infected with each virus at an MOI of 10 in infection medium without TPCK-treated trypsin for 1 hour. Then the media were replaced with 0.3 ml medium supplemented with 5% fetal calf serum (FCS), 1% penicillin-streptomycin (P/S), and 1% vitamins, and buffered with 25 mM HEPES. After 6 hours post-infection (hpi), cells were treated with 0.3 mL infection medium containing 5 μg/mL TPCK-treated trypsin for 15 min. Each well was washed twice with 1 mL of citric acid-adjusted PBS at a series of pH range from 5.0 to 6.1 (with 0.1 pH units change) and incubated for 5 min at 37 °C. Cells were incubated in 0.3 mL MEM containing 5% FBS for 3 hours at 37 ˚C. When syncytium formation was identified microscopically, the cells were fixed and stained with the differential quick staining kit (Electron Microscopy Sciences, PA, USA). The pH of activation was recorded as the highest pH at which syncytia were observed.

Viral replication kinetics *in vitro*. Confluent MDCK and NPTr cells in 12-well plates were washed twice with PBS before inoculation. The cells were inoculated at a multiplicity of infection (MOI) of 0.001 in 1 mL infection medium, with two repeats. Supernatants were collected at 0, 2, 12, 24, 36, 48, 60 and 72 hpi and were titrated on MDCK cells in 6-well plate by plaque assay.

Preparation of swine trachea and lung explants. Intact respiratory tracts were obtained from 6-month-old pigs (*Sus Scrofa domestica*) in Sheung Shui Slaughterhouse, Hong Kong, and delivered to the laboratory

within 3 hours. Prior to explant isolation, a tracheal swab was taken for real-time PCR detection of influenza A virus matrix (M) gene. If positive, data from that particular set were discarded. Isolation and culturing of the explants were as previously described with slight modifications[44-46]. To prepare tracheal explants, the tracheal tube was excised from the respiratory tract, rinsed in washing medium and cut open. The epithelial layer was carefully removed from the cartilage and punched into similar size with a disposable 5 mm biopsy punch (Integra York PA Inc, York, USA). Each tracheal explant was put onto a surgical sponge (Simport Scientific, Quebec, Canada) with its epithelial surface facing upward and floating in a 12-well tissue culture plate filled with 1.5 mL culture medium to create an air-liquid interface (ALI). The culture medium contained 50% RPMI 1640, 50% DMEM high glucose, 100 U/mL penicillin, 100 µg/mL streptomycin, 0.1 mg/mL gentamicin and 0.3 mg/mL glutamine (Gibco, New York, USA). To prepare the lung explants, the intermediate lung lobe was chosen for explant isolation. Using a 4.0 mm Ruschelit tracheal tube (Teleflex, North Carolina, USA) the lobe was perfused with cold washing medium. The washing medium was aspirated, and the lobe was inflated with 1% low gelling temperature agarose (Sigma-Aldrich, Missouri, USA) in PBS. As the gel was solidified, the inflated lobe was dissected into smaller rectangle cubes and embedded in 4% low gelling temperature agarose. A cryotome blade was used to cut the embedded lung tissues into thin slices of <1 mm thick, which was further punched into similar size with a disposable 5 mm biopsy punch and put on surgical sponges in culture medium as described in tracheal explant isolation. The culture medium contained DMEM high glucose, 100 U/mL penicillin, 100 µg/mL streptomycin, 0.1 mg/mL gentamicin, 0.5 µg/ml hydrocortisone (Sigma-Aldrich, Missouri, USA), 0.5 µg/mL vitamin A (Sigma-Aldrich, Missouri, USA), and 2.5 µg/mL bovine insulin (Sigma-Aldrich, Missouri, USA).

Infection of swine lung and trachea explants. Prior to infection, prepared tracheal explants were cultured at 37^{o}C, while lung explants were cultured at 39^{o}C according to swine natural physiological temperature, in humidified incubators with 5% CO_2. Medium was changed at 1 hour period during the first 3 hours after isolation. For infection (24 h after explants were prepared), tissue explants were submerged in 1 mL virus stock with titres of 10^5 pfu/mL for 1 hour at 37^{o}C in humidified incubators with 5% CO_2. Tissue explants were washed with PBS to remove unbound viruses. Each tissue explant was placed onto a surgical sponge with its epithelial surface facing upward in a 12-well tissue culture plate filled with 1.5 mL/well of the corresponding culture medium. Tracheal explants were cultured at 37^{o}C, while lung explants were cultured at 39^{o}C, in humidified incubators with 5% CO_2. Culture supernatant was collected at 1, 24, 48 and 72 hpi for viral load quantification using plaque assay on MDCK cells in 6-well plates. The experiments were performed in three full complete, independent biological replicates.

Site-directed mutagenesis. Primers designed via QuickChange Primer Design (https://www.agilent.com/store/primerDesignProgram.jsp) were used to introduce specific mutations to HA, PB1, NP genes. The PCR reactions were performed using QuickChange Multi Site-Directed Mutagenesis Kit in accordance with the manufacturer's instructions (Agilent, Santa Clara, USA).

Minigenome assay. The polymerase activity was evaluated by minigenome assay[23,24]. In brief, 1 μg of each polymerase gene plasmid, 2 μg of NP plasmid, 1 μg reporter plasmid encoding the codon firefly luciferase flanked by the non-coding region of influenza M gene either driven by human Polymerase I promoter[47] or swine Polymerase I promoter[48] and 0.1 μg phRL-CMV plasmid (renilla luciferase driven by CMV promotor) were transfected respectively into 293T cells or NPTr cells in the 6-well plates by using TransIT (MIRUS, Madison, USA) reagent according to the manufacturer's recommendation protocol. After 24 hours, the luciferase activity was measured with the dual-luciferase reporter system (Promega, Madison, WI, USA) on a SpectraMax iD5 Multi-Mode Microplate Reader (Molecular Devices, San Jose, USA).

Ethics Statements. All pig transmission experiment were performed in an ABSL2+ facility at St. Jude Children Research Hospital, in compliance with the NIH and the animal Welfare and with the approval of the St. Jude Animal Care and Use Committee (Protocol 428).

Transmissibility of EA swine influenza viruses in pigs. Yorkshire Crossbred piglets (Midwest Research Swine LLC., Glencoe, MN USA) at 3 to 4 weeks old were used in the study. Prior to the experiments, pigs were confirmed as seronegative for influenza A virus NP protein (ID.vet, Grabels, France) and showed HI titer $\leq$ 1:10 for the homologous EA swine influenza virus. Two donor pigs were inoculated intranasally with 10^6 pfu in 1 mL PBS under anesthesia and two naïve pigs were each introduced to co-house with two donors on 1 day post-inoculation (dpi). Each virus was tested in duplicates with a total of four donors and four direct contacts. Nasal swabs from all donor pigs were collected from both nostrils on 2, 4, 6, 8 and 10 or 11 dpi. Donors were euthanized on 11 dpi for post-infection sera collection. Nasal swabs from all contact pigs were collected from both nostrils on 1, 3, 5, 7, 9, 10 and 11 or 13 days post-exposure (dpe). Contact pigs were euthanized on 10 or 13 dpe for post-exposure sera collection. All nasal swabs were placed into 1 mL of viral transport medium (VTM) and stored at -80 ^{o}C. Infectious viral titers in the nasal swabs were determined by $TCID_{50}$ assay.

Hemagglutination inhibition (HI) assay. Antibodies against the homologous virus from donor or contact pigs were tested by HI assay following standard procedures. Post-sera were collected from donor pigs on 11 dpi or from contact pigs on 10 or 13 dpe. In brief, pig sera were treated with receptor-destroying enzyme, RDE (Denka Seiken Tokyo, Japan), for 18-20 hours in a 37^{o}C water-bath and then inactivated for 30 min at 56^{o}C. The final dilution of RDE-treated sera is 1:10. After preparing two-fold serial dilution in 96-well V-bottom microplate, the corresponding virus at the volume of 25 μL containing 4 HA Units was added into the plates and then incubated for 30 min at room temperature. Subsequently, 50μL of 0.5% Turkey red blood cells was added, and the plate was slightly shaken and incubated at room temperature for 30 min. HI titers were expressed as the highest dilution of serum that completely inhibited agglutination of virus and erythrocytes. The detection limit was 1:10. Seroconversion was applied using HI titre $\geq$1:20 as the cut-off value.

Sequence analysis. H1N1 subtype swine influenza viruses and avian influenza viruses were downloaded from NCBI and Global Initiative on Sharing All Influenza Data (GISAID, https://www.gisaid.org/). The

sequences that clustered with the gene segments of A/duck/Bavaria/1/1977 (H1N1) were extracted from these maximum likelihood phylogenetic trees. Finally, eight gene segments, PB2 (N = 417), PB1 (N = 381), PA (N = 382), HA (N = 454), NP (N = 495), NA (N = 429), M (N = 396), NS (N = 391) of EA swine influenza viruses isolated from 1979 to 2016 were used for specific amino acids prevalence analysis. To investigate if mutations (i.e. PB1-Q621R and NP-R351K) are conserved among influenza A viruses, the PB1 of 74,095 influenza A viruses and NP of 80,188 influenza A viruses isolated from 1933 to 2019, respectively, were downloaded from GISAID. Sequences were aligned using MAFFT[49] at the CIPRES science gateway (Version 3) (https://www.phylo.org/)[50]. The number of amino acids were counted using BioEdit (Version 7.0).

Serial passages *in vitro* and *in ovo*. To compare for mutations that may emerge after passaging in vitro and in ovo, recombinant viruses RG-Be02-lung^{SG}xEA2^{IG}, RG-EA1, RG-EA2, RG-EA3, RG-EA4 were serial passaged in MDCK cells, NPTr cells, and in 10-day old embryonated chicken eggs using transfection supernatant as starting materials. Infections *in vitro* were performed using MOI of 0.001-0.005 at each passage and infections *in ovo* were performed using 10^4 pfu in 0.1 mL. Three independent serial passages were performed in parallel for each experimental condition. Culture supernatant or allantoic fluid harvested from passage one (P1) and passage three (P3) were analysed by next generation sequencing.

Next-Generation Sequencing. Nasal swabs with peak virus titers collected from the indicated contact pigs were analysed by next generation sequencing. Briefly, viral RNA was extracted from swabs with peak virus titers by using QIAamp viral RNA mini kit (Qiagen, Hilden, Germany). RNA was transcribed into cDNA with SuperScript^{TM} III Reverse Transcriptase (Invitrogen, California, USA). The gene segments were amplified by Q5 High Fidelity DNA polymerase (NEB, Massachusetts, USA) using a pair of primers (454-Tag1-U12:GCC GGA GCT CTG CAG ATA TCA GCR AAA GCA GG; 454-Tag1-U13:GCC GGA GCT CTG CAG ATA TCA GTA GAA ACA AGG). Libraries were prepared based on the Nextera DNA Flex Library Preparation standard protocol[51]. 300ng PCR products were cleaved and tagged by bead-linked transposome at 55^{o}C, then the tagmented DNA were amplified with a pair of indexes using a 5-cycle PCR program. The amplified libraries were further purified by using 1 volume of sample purification beads. The libraries were finally eluted using 32 µL resuspension buffer. The purified libraries were quantified with Agilent fragment analyzer automated CE system with the high sensitivity NGS fragment analysis 474 kit (Agilent, California, USA). 150 pM pool library containing index adapters allowing multiplex sequencing of 4 samples per iSeq 100 i1 Cartridge was run on iseq100 sequencing system (Illumnia, California, USA). All data were analysed on CLC Genomic workbench (version 20) (Qiagen, Hilden, Germany) using 1% as variant calling threshold. The nucleotide substitutions with a frequency of 5% or more were further analysed.

NA kinetics. NA kinetics analysis was performed in a flat-bottom 96-well opaque black plate (PerkinElmer, Waltham, MA, USA) as described previously[52]. Briefly, each virus at 10^7 pfu/mL was added into various 2'-(4-Methylumbelliferyl)-α-D-*N*-acetylneuraminic acid (MUNANA) (Sigma-Aldrich, Missouri, USA)

substrate concentrations. Fluorescence was monitored every 68 s for 60 min at 37 °C in a microplate reader, using excitation and emission wavelengths of 355 and 460 nm, respectively. Time course data from each concentration of the MUNANA substrate were plotted by linear regression analysis. Data with R^2>0.99 were used for kinetic parameters analysis. Enzyme kinetics data were fitted to the Michaelis–Menten equation by using nonlinear regression (Prism, GraphPad, version 8.4.1) to determine the Michaelis constant and maximum velocity (V_{max}) of substrate conversion.

Immunofluorescence staining for influenza NP. To investigate the effect of mutation in NP on cellular distribution of NP during the virus life cycle, NPTr cells were infected with virus at an MOI of 5. Infections were stopped at 2, 4, 6, 8, 10 and 12 hpi by fixation in 4% paraformaldehyde (Electron Microscopy Sciences, PA, USA). The cells were then permeabilized with 0.1% Triton™ X-100 in PBS for 30 min. After blocking with 10% BSA blocking serum in PBS, the cells were labelled with 1:200 dilution of mouse monoclonal IgG2a Influenza A NP antibody (Santa Cruz Biotech, Inc, Santa Cruz, USA) at 4 ˚C overnight. After three washes, the cells were subsequently incubated with a 1:200 dilution of FITC Goat Anti-Mouse IgG/IgM (BD Pharmingen™, San Jose, USA) for 3 hours at room temperature in the dark. After three washes, the nuclei were counterstained at a 1:1000 dilution of DAPI (4',6'-diamidino-2-phenylindole) in SlowFade™ Gold Antifade Mountant (Thermo Fisher Scientific, Eugene, USA) at room temperature for 15 min. Cell imaging and fluorescence were carried out using the Nikon Eclipse Ti-S fluorescence microscope (Nikon, Tokyo, Japan) equipped with a Nikon DS-Qi2 camera and the iNIS-Elements BR imaging software (Version 4.40). The positive cells were numerated using FIJI[53].

Statistical Analyses. One-way ANOVA was used to compare multiple groups and two-way ANOVA was used to compare virus titers over time, followed by Tukey's multiple comparisons post-hoc tests. Area under the curve was calculated from the nasal swabs of the donor and contact pigs. Two-sided Mann-Whitney test was performed to compare two groups, and Kruskal-Wallis test and Dunn's multiple comparisons post hoc test were used to compare multiple groups. Spearman's rank correlation coefficient analysis was performed for the monotonic relationship between virus replication efficiency and viral transmissibility. Data were analyzed in Microsoft Excel for Mac, version 16.28 and GraphPad Prism version 8.4.1 for Windows (GraphPad Software, La Jolla, USA). Statistically significant *P* values are indicated as * $P < 0.05$, ** $P < 0.01$. All statistical parameters for specific analyses are shown in the corresponding figure legends.

Declarations

ACKNOWLEDGMENTS

We thank the St. Jude core facilities, including the Animal Resources Centre and the Veterinary Pathology Core for technical support. This study was supported by Contract HHSN272201400006C from NIAID, NIH, USA, the Theme-Based Research Scheme (T11-705/14N) from the Research Grants Council, Hong Kong SAR, China. YCFS, UJ, JJ and GJDS are supported by the Duke-NUS Signature Research Programme funded by the Ministry of Health, Singapore.

Author contributions: H.L.Y., G.J.D.S. and R.J.W. conceived and designed the experiments; W.S., Y.C.F.S., U.J., J.J. and G.J.D.S. performed sequences analysis; W.S., Y.Z., Y.J., and M.T.Z. performed experiments *in vitro*; W.S. and C.L. performed experiments *ex vivo*. W.S., R.H., J.D.B., J.C.C., T.J., A.R., J.F., P.N.Q.P., C.K., J.C.J., and L.K. performed animal experiments *in vivo*; S.K., S.P., M.C.W.C., R.G.W., C.Y.W., K.V.R. and M.P. provided novel reagents to support the study. W.S., Y.C.F.S., G.J.D.S., R.J.W., M.P. and H.L.Y. wrote the draft manuscript and all authors reviewed the paper.

Competing interests: The authors declare no competing interests.

Data availability:

Sequences of Sanger sequencing have been deposited to the public database GISAID under the following accession number. A/duck/Bavaria/2/1977: EPI_ISL_539860; A/swine/Arnsberg/6554/1979: EPI_ISL_539869; A/swine/Belgium/1/1979: EPI_ISL_1055769; A/swine/Belgium/2/1979: EPI_ISL_1055773; A/swine/Netherlands/3/1980: EPI_ISL_539861; A/swine/Germany/2/1981: EPI_ISL_539862; A/swine/Netherlands/12/1985: EPI_ISL_539863; A/swine/Italy/670/1987: EPI_ISL_68983; A/swine/Schleswig-Holstein/1/1992: EPI_ISL_539864; A/swine/Hong Kong/8512/2001: EPI_ISL_539865; A/swine/Hong Kong/72/2007 EPI_ISL_539866; A/swine/Hong Kong/1559/2008: EPI_ISL_539867; A/swine/Hong Kong/NS29/2009: EPI_ISL_29774; A/swine/Hong Kong/NS4848/2011: EPI_ISL_539868; RG-EA1: EPI_ISL_539852; RG-EA2: EPI_ISL_539853; RG-EA3: EPI_ISL_539854; RG-EA4: EPI_ISL_539855; A/swine/Belgium/1/1979: EPI_ISL_1055769); A/swine/Belgium/2/1979: EPI_ISL_1055773. Samples of next generation sequencing have been deposited in the Sequence Read Archive of the NCBI, under project accession number PRJNA725802. All other data shown in figures 1, 2, 3, 4, 5 and supplementary figure 1 are available from the corresponding author upon reasonable request. Source data are provided with this paper.

References

1 Kuiken, T. *et al.* Host species barriers to influenza virus infections. *Science* **312**, 394-397, doi:10.1126/science.1122818 (2006).

2 Parrish, C. R. *et al.* Cross-species virus transmission and the emergence of new epidemic diseases. *Microbiol. Mol. Biol. Rev.* **72**, 457-470, doi:10.1128/mmbr.00004-08 (2008).

3 Taubenberger, J. K. & Kash, J. C. Influenza virus evolution, host adaptation, and pandemic formation. *Cell Host Microbe* **7**, 440-451, doi:10.1016/j.chom.2010.05.009 (2010).

4 Lipsitch, M. *et al.* Viral factors in influenza pandemic risk assessment. *Elife* **5**, doi:10.7554/eLife.18491 (2016).

5 Long, J. S., Mistry, B., Haslam, S. M. & Barclay, W. S. Host and viral determinants of influenza A virus species specificity. *Nat. Rev. Microbiol.* **17**, 67-81, doi:10.1038/s41579-018-0115-z (2019).

6 Smith, G. J. *et al.* Origins and evolutionary genomics of the 2009 swine-origin H1N1 influenza A epidemic. *Nature* **459**, 1122-1125, doi:10.1038/nature08182 (2009).

7 WHO. *Influenza—Avian and other zoonotic influenza 2020*, <https://www.who.int/influenza/human_animal_interface/en/> (2020).

8 Pensaert, M., Ottis, K., Vandeputte, J., Kaplan, M. M. & Bachmann, P. A. Evidence for the natural transmission of influenza A virus from wild ducts to swine and its potential importance for man. *Bull. World Health Organ.* **59**, 75-78 (1981).

9 Brown, I. H. History and epidemiology of Swine influenza in Europe. *Curr Top Microbiol. Immunol.* **370**, 133-146, doi:10.1007/82_2011_194 (2013).

10 Krumbholz, A. *et al.* Origin of the European avian-like swine influenza viruses. *J. Gen. Virol.* **95**, 2372-2376, doi:10.1099/vir.0.068569-0 (2014).

11 Joseph, U., Vijaykrishna, D., Smith, G. J. D. & Su, Y. C. F. Adaptive evolution during the establishment of European avian-like H1N1 influenza A virus in swine. *Evol. Appl.* **11**, 534-546, doi:10.1111/eva.12536 (2018).

12 Vijaykrishna, D. *et al.* Long-term evolution and transmission dynamics of swine influenza A virus. *Nature* **473**, 519-522, doi:10.1038/nature10004 (2011).

13 Yang, H. *et al.* Prevalence, genetics, and transmissibility in ferrets of Eurasian avian-like H1N1 swine influenza viruses. *Proc. Natl. Acad. Sci. USA* **113**, 392-397, doi:10.1073/pnas.1522643113 (2016).

14 Henritzi, D. *et al.* Surveillance of European Domestic Pig Populations Identifies an Emerging Reservoir of Potentially Zoonotic Swine Influenza A Viruses. *Cell Host Microbe* **28**, 614-627.e616, doi:10.1016/j.chom.2020.07.006 (2020).

15 Dornfeld, D., Petric, P. P., Hassan, E., Zell, R. & Schwemmle, M. Eurasian Avian-Like Swine Influenza A Viruses Escape Human MxA Restriction through Distinct Mutations in Their Nucleoprotein. *J. Virol.* **93**, doi:10.1128/JVI.00997-18 (2019).

16 Sun, H. *et al.* Prevalent Eurasian avian-like H1N1 swine influenza virus with 2009 pandemic viral genes facilitating human infection. *Proc. Natl. Acad. Sci. USA* **117**, 17204-17210, doi:10.1073/pnas.1921186117 (2020).

17 Thornton, J. W., Need, E. & Crews, D. Resurrecting the ancestral steroid receptor: ancient origin of estrogen signaling. *Science* **301**, 1714-1717, doi:10.1126/science.1086185 (2003).

18 Ducatez, M. F. *et al.* Feasibility of reconstructed ancestral H5N1 influenza viruses for cross-clade protective vaccine development. *Proc. Natl. Acad. Sci. USA* **108**, 349-354, doi:10.1073/pnas.1012457108 (2011).

19 Rogers, G. N. & Paulson, J. C. Receptor determinants of human and animal influenza virus isolates: differences in receptor specificity of the H3 hemagglutinin based on species of origin. *Virology* **127**, 361-373, doi:10.1016/0042-6822(83)90150-2 (1983).

20 Baumann, J., Kouassi, N. M., Foni, E., Klenk, H. D. & Matrosovich, M. H1N1 Swine Influenza Viruses Differ from Avian Precursors by a Higher pH Optimum of Membrane Fusion. *J. Virol.* **90**, 1569-1577, doi:10.1128/JVI.02332-15 (2016).

21 Russier, M. *et al.* H1N1 influenza viruses varying widely in hemagglutinin stability transmit efficiently from swine to swine and to ferrets. *PLoS Pathog.* **13**, e1006276, doi:10.1371/journal.ppat.1006276 (2017).

22 Pleschka, S. *et al.* A plasmid-based reverse genetics system for influenza A virus. *J. Virol.* **70**, 4188-4192, doi:10.1128/JVI.70.6.4188-4192.1996 (1996).

23 Salomon, R. *et al.* The polymerase complex genes contribute to the high virulence of the human H5N1 influenza virus isolate A/Vietnam/1203/04. *J. Exp. Med.* **203**, 689-697, doi:10.1084/jem.20051938 (2006).

24 Thornton, J. W. Resurrecting ancient genes: experimental analysis of extinct molecules. *Nat. Rev. Genet.* **5**, 366-375, doi:10.1038/nrg1324 (2004).

25 Giles, B. M. & Ross, T. M. A computationally optimized broadly reactive antigen (COBRA) based H5N1 VLP vaccine elicits broadly reactive antibodies in mice and ferrets. *Vaccine* **29**, 3043-3054, doi:10.1016/j.vaccine.2011.01.100 (2011).

26 Shi, Y., Wu, Y., Zhang, W., Qi, J. & Gao, G. F. Enabling the 'host jump': structural determinants of receptor-binding specificity in influenza A viruses. *Nat. Rev. Microbiol.* **12**, 822-831, doi:10.1038/nrmicro3362 (2014).

27 Matrosovich, M. *et al.* Early alterations of the receptor-binding properties of H1, H2, and H3 avian influenza virus hemagglutinins after their introduction into mammals. *J. Virol.* **74**, 8502-8512, doi:10.1128/jvi.74.18.8502-8512.2000 (2000).

28 Taubenberger, J. K. & Morens, D. M. The 1918 Influenza Pandemic and Its Legacy. *Cold Spring Harb. Perspect. Med.* **10**, doi:10.1101/cshperspect.a038695 (2020).

29 Reid, A. H., Fanning, T. G., Janczewski, T. A., Lourens, R. M. & Taubenberger, J. K. Novel origin of the 1918 pandemic influenza virus nucleoprotein gene. *J. Virol.* **78**, 12462-12470, doi:10.1128/jvi.78.22.12462-12470.2004 (2004).

30 Davey, J., Dimmock, N. J. & Colman, A. Identification of the sequence responsible for the nuclear accumulation of the influenza virus nucleoprotein in Xenopus oocytes. *Cell* **40**, 667-675, doi:10.1016/0092-8674(85)90215-6 (1985).

31 Wang, P., Palese, P. & O'Neill, R. E. The NPI-1/NPI-3 (karyopherin alpha) binding site on the influenza a virus nucleoprotein NP is a nonconventional nuclear localization signal. *J. Virol.* **71**, 1850-1856, doi:10.1128/jvi.71.3.1850-1856.1997 (1997).

32 Weber, F., Kochs, G., Gruber, S. & Haller, O. A classical bipartite nuclear localization signal on Thogoto and influenza A virus nucleoproteins. *Virology* **250**, 9-18, doi:10.1006/viro.1998.9329 (1998).

33 Ye, Q., Krug, R. M. & Tao, Y. J. The mechanism by which influenza A virus nucleoprotein forms oligomers and binds RNA. *Nature* **444**, 1078-1082, doi:10.1038/nature05379 (2006).

34 Gabriel, G. *et al.* Differential use of importin-α isoforms governs cell tropism and host adaptation of influenza virus. *Nat. Commun.* **2**, 156, doi:10.1038/ncomms1158 (2011).

35 Zimmermann, P., Mänz, B., Haller, O., Schwemmle, M. & Kochs, G. The viral nucleoprotein determines Mx sensitivity of influenza A viruses. *J. Virol.* **85**, 8133-8140, doi:10.1128/jvi.00712-11 (2011).

36 Mänz, B. *et al.* Pandemic influenza A viruses escape from restriction by human MxA through adaptive mutations in the nucleoprotein. *PLoS Pathog.* **9**, e1003279, doi:10.1371/journal.ppat.1003279 (2013).

37 Ashenberg, O., Padmakumar, J., Doud, M. B. & Bloom, J. D. Deep mutational scanning identifies sites in influenza nucleoprotein that affect viral inhibition by MxA. *PLoS Pathog.* **13**, e1006288, doi:10.1371/journal.ppat.1006288 (2017).

38 Stamatakis, A. RAxML version 8: a tool for phylogenetic analysis and post-analysis of large phylogenies. *Bioinformatics* **30**, 1312-1313, doi:10.1093/bioinformatics/btu033 (2014).

39 Finnigan, G. C., Hanson-Smith, V., Stevens, T. H. & Thornton, J. W. Evolution of increased complexity in a molecular machine. *Nature* **481**, 360-364, doi:10.1038/nature10724 (2012).

40 Tamuri, A. U. Treesub: annotating ancestral substitution on a tree.Available at: https://github.com/tamuri/treesub (2013) (Accessed June 12, 2018).

41 Stech, J. *et al.* Rapid and reliable universal cloning of influenza A virus genes by target-primed plasmid amplification. *Nucleic Acids Res.* **36**, e139, doi:10.1093/nar/gkn646 (2008).

42 Hoffmann, E., Neumann, G., Kawaoka, Y., Hobom, G. & Webster, R. G. A DNA transfection system for generation of influenza A virus from eight plasmids. *Proc. Natl. Acad. Sci. USA* **97**, 6108-6113, doi:10.1073/pnas.100133697 (2000).

43 Su, W. *et al.* Testing the Effect of Internal Genes Derived from a Wild-Bird-Origin H9N2 Influenza A Virus on the Pathogenicity of an A/H7N9 Virus. *Cell Rep.* **12**, 1831-1841, doi:10.1016/j.celrep.2015.08.029 (2015).

44 Van Poucke, S. G., Nicholls, J. M., Nauwynck, H. J. & Van Reeth, K. Replication of avian, human and swine influenza viruses in porcine respiratory explants and association with sialic acid distribution. *Virol. J.* **7**, 38, doi:10.1186/1743-422X-7-38 (2010).

45 Chan, R. W. *et al.* Infection of swine ex vivo tissues with avian viruses including H7N9 and correlation with glycomic analysis. *Influenza Other Respir. Viruses* **7**, 1269-1282, doi:10.1111/irv.12144 (2013).

46 Chan, L. L. Y. *et al.* Evaluation of the human adaptation of influenza A/H7N9 virus in PB2 protein using human and swine respiratory tract explant cultures. *Sci. Rep.* **6**, 35401, doi:10.1038/srep35401 (2016).

47 Hoffmann, E., Neumann, G., Hobom, G., Webster, R. G. & Kawaoka, Y. "Ambisense" approach for the generation of influenza A virus: vRNA and mRNA synthesis from one template. *Virology* **267**, 310-317, doi:10.1006/viro.1999.0140 (2000).

48 Moncorge, O. *et al.* Investigation of influenza virus polymerase activity in pig cells. *J. Virol.* **87**, 384-394, doi:10.1128/JVI.01633-12 (2013).

49 Katoh, K., Misawa, K., Kuma, K. & Miyata, T. MAFFT: a novel method for rapid multiple sequence alignment based on fast Fourier transform. *Nucleic Acids Res.* **30**, 3059-3066, doi:10.1093/nar/gkf436 (2002).

50 M. A. Miller, W. P., T. Schwartz. in *Gateway Computing Environments Workshop.* Vol. 23 1-8 (IEEE, New Orleans, LA, USA, 2010).

51 Bruinsma, S. *et al.* Bead-linked transposomes enable a normalization-free workflow for NGS library preparation. *BMC Genomics* **19**, 722, doi:10.1186/s12864-018-5096-9 (2018).

52 Yen, H.-L. *et al.* Hemagglutinin–neuraminidase balance confers respiratory-droplet transmissibility of the pandemic H1N1 influenza virus in ferrets. *Proc. Natl. Acad. Sci. USA* **108**, 14264-14269, doi:10.1073/pnas.1111000108 (2011).

53 Schindelin, J. *et al.* Fiji: an open-source platform for biological-image analysis. *Nat. Methods* **9**, 676-682, doi:10.1038/nmeth.2019 (2012).

Figures

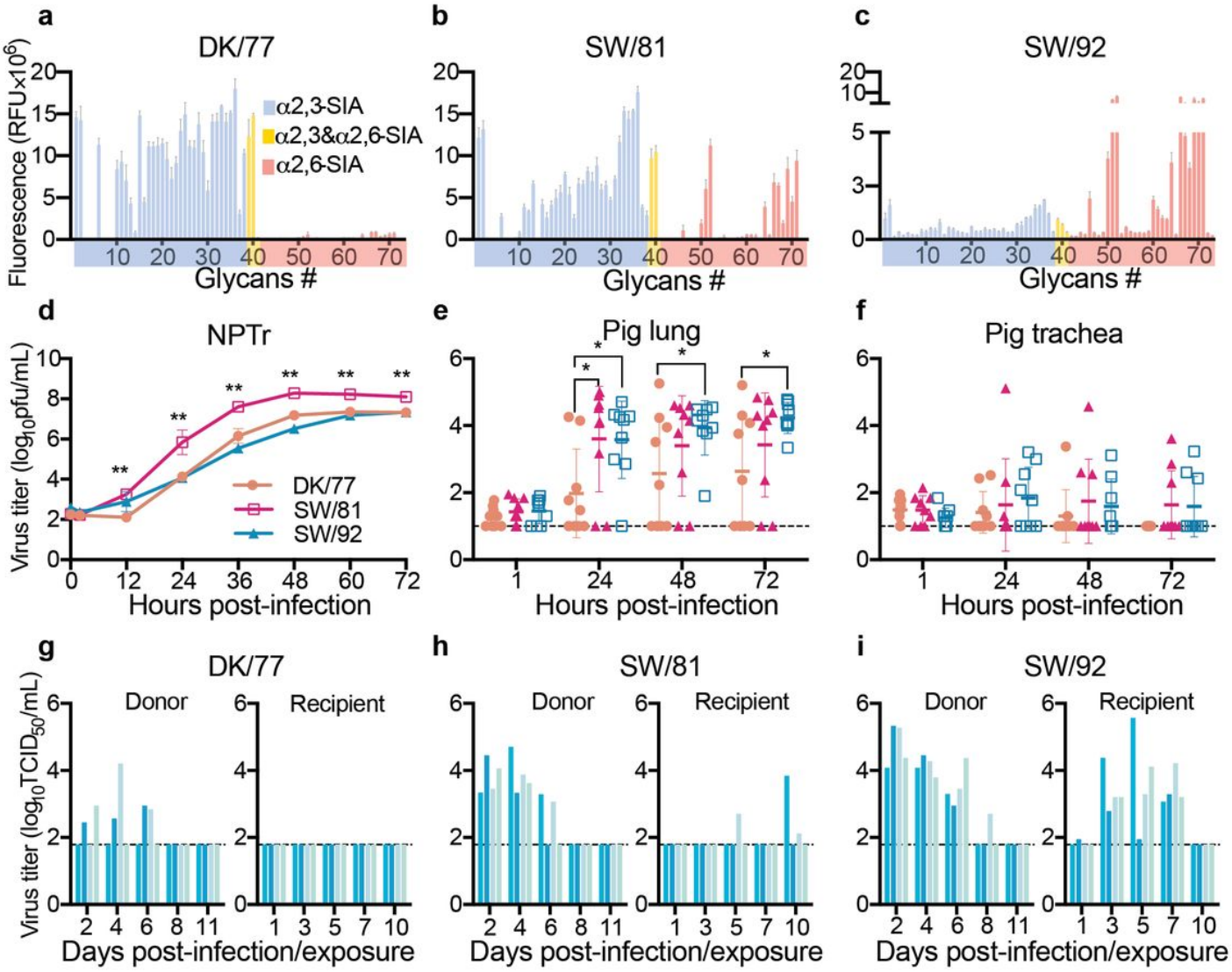


Figure 1

Avian and EA swine influenza viruses differed in receptor binding profiles, replication efficiency in vitro and ex vivo, and contact transmissibility in pigs. a,b,c, Glycan array analysis of avian influenza virus DK/77 (a) and EA swine influenza viruses SW/81 (b) and SW/92 (c). Glycan array data are shown with the mean and SD fluorescence (RFU) calculated from 6 replicate spots of each glycan. d, Multicycle replication kinetics in NPTr cells. Mean and SD from three repeats in one of two independently performed experiment are shown. Statistical differences were calculated by two-way ANOVA followed by a Tukey's multiple comparisons post-hoc test. *P < 0.05, **P < 0.01. e,f, Replication kinetics in pig lung (e) and pig trachea (f) ex vivo cultures. Tissues from three healthy pigs were used to prepare lung (N=3 per pig) and tracheal (N=3 per pig) explants for the experiments. Each data point represents one explant sample. Mean and SD from 9 data points are shown. Statistical differences were calculated by two-way ANOVA followed by a Tukey's multiple comparisons post-hoc test. *P < 0.05. g,h,i, Contact transmissibility of DK/77 avian influenza virus (g), SW/81 (h), and SW/92 (i) EA swine influenza viruses in pigs. Each virus was tested in duplicate with a total of four donors and four direct contacts. Pigs housed in the same pen

are denoted by the same colour. The limit of detection (1.789 log10TCID50/mL) is shown with the horizontal dashed line.

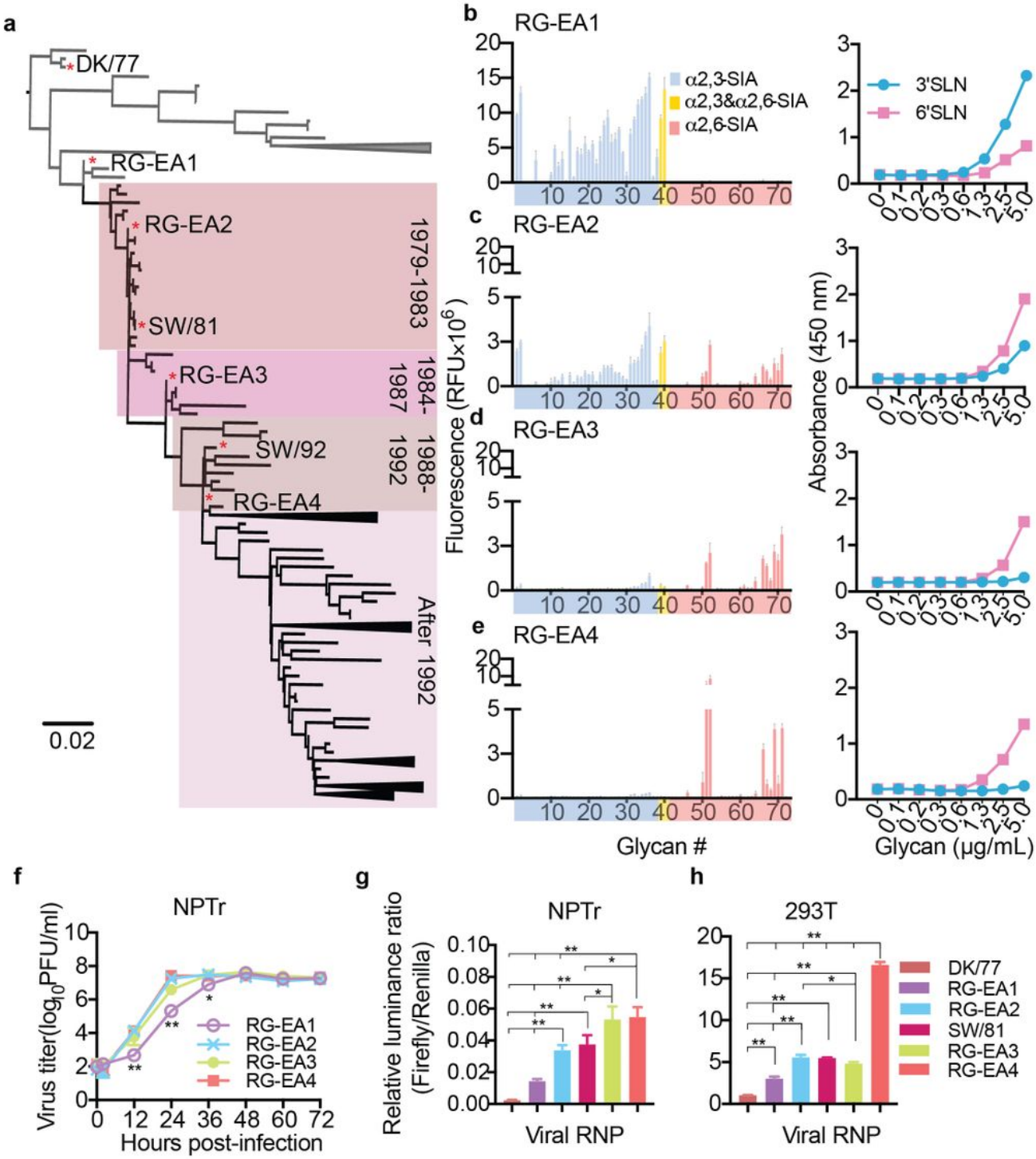


Figure 2

Characterization of resurrected EA influenza viruses representing different evolutionary stages of EA swine influenza viruses. a, The maximum likelihood phylogeny of HA gene sequences was constructed using avian (N = 69) and EA swine viruses (N = 344) isolated from 1977 to 2014. The phylogenetic tree

was rooted to the branch of A/duck/Bavaria/2/1977 (H1N1) (DK/77). b,c,d,e, Receptor binding profiles of resurrected RG-EA1 (b), RG-EA2 (c), RG-EA3 (d), RG-EA4 (e) viruses. Glycan array data (left panel) are shown with the mean and SD fluorescence (RFU) calculated from 6 replicate spots of each glycan (left panel), and the enzyme-linked immunosorbent assay (right panel) results are shown with the mean and SD absorbance (450 nm) from 3 replicates in one of two independently performed experiment. f, Multicycle replication kinetics in NPTr cells. Mean and SD from three repeats in one of two independently performed experiment is shown. Statistical differences were calculated by two-way ANOVA followed by a Tukey's multiple comparisons post-hoc test. *P < 0.05, **P < 0.01. g,h, Polymerase activity in NPTr cells (g) and 293T cells (h). The mean and SD ratio of firefly/ renilla luciferase from three repeats in one of two independently performed experiment is shown. One-way ANOVA with Tukey's multiple comparison test was performed and significant differences are labelled: *P < 0.05 and **P < 0.01.

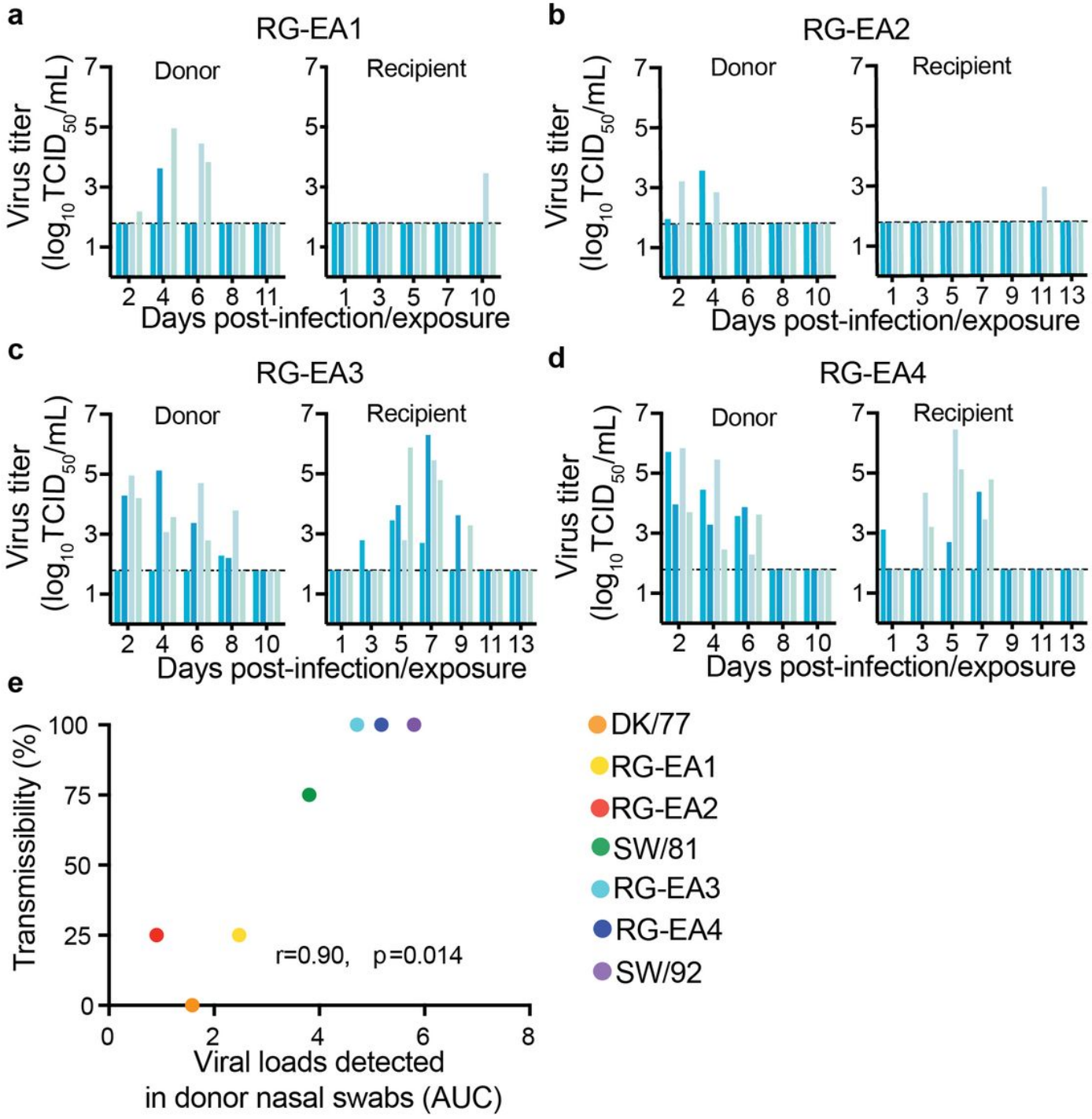


Figure 3

EA swine H1N1 viruses acquired efficient pig-to-pig transmissibility after 1983. a, b, c, d, The transmissibility of the four resurrected viruses RG-EA1 (a), EA2 (b), EA3 (c), and EA4 (d) in pigs. Contact transmission experiments were performed in duplicate with a total of four donors and four direct contacts. Pigs housed in the same pen are denoted by the same colour. The limit of detection (1.789 log10TCID50/mL) is shown with the horizontal dashed line. e, Spearman's rank correlation coefficient analysis was used to evaluate the correlation between viral loads detected in donor nasal swabs (mean

AUC from 4 pigs, X axis) and onward transmissibility (% of infected out of 4 exposed contact pigs, Y axis).

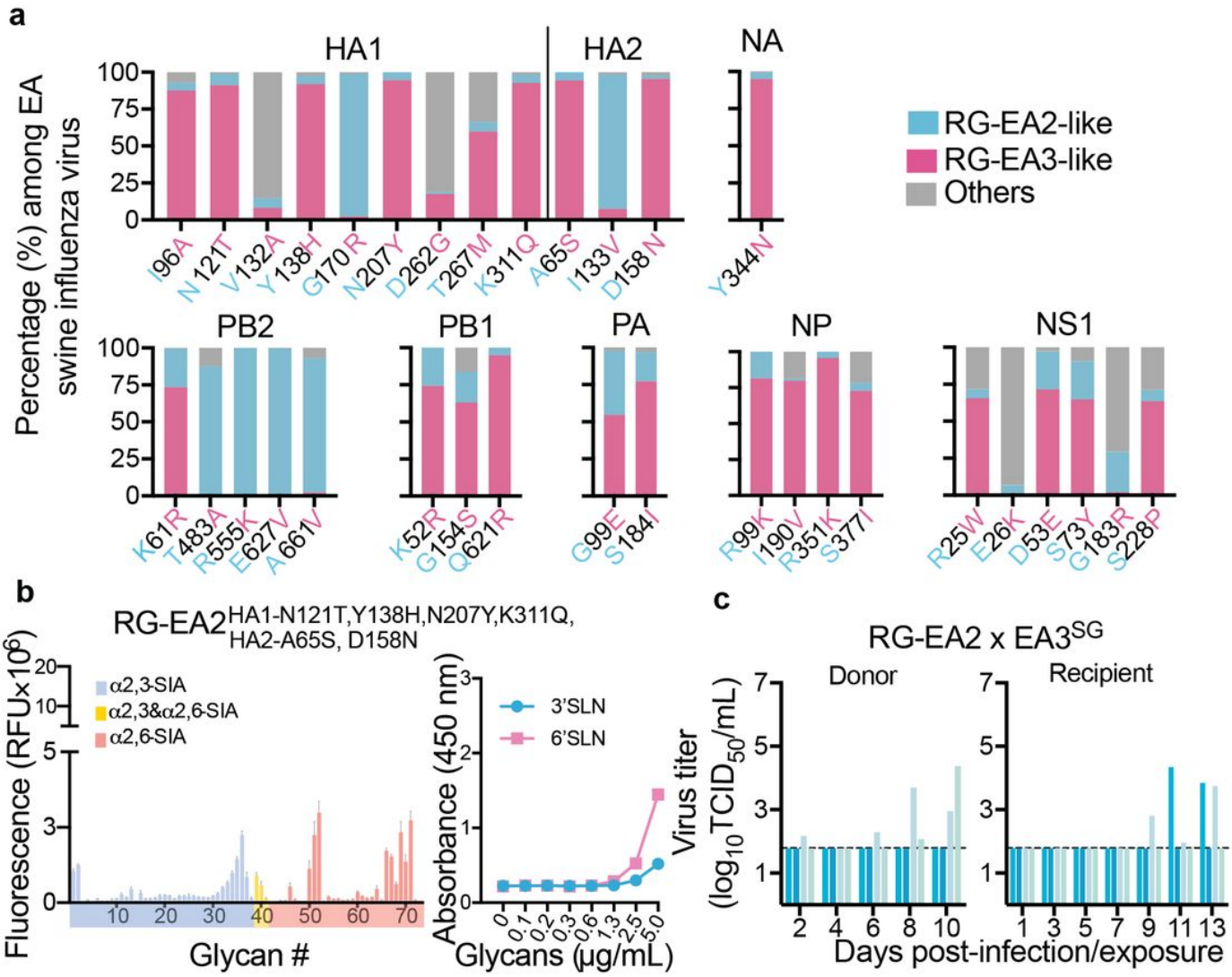


Figure 4

Introducing HA and NA genes derived from RG-EA3 virus did not enhance efficient contact transmissibility of RG-EA2 virus in pigs. a, The detection frequency of the 33 amino acids that differed between RG-EA2 and RG-EA3 EA swine viruses among PB2 (N = 417), PB1 (N = 381), PA (N = 382), HA1/HA2 (N = 454), NP (N = 495), NA (N = 429), NS1 (N = 391) of EA swine influenza A viruses isolated in 1979-2016 were analyzed. Amino acid residues that resembled RG-EA2, RG-EA3, or other amino acids are colored in cyan, magenta, and gray, respectively. HA and NA are numbered according to H1 and N1 numbering, respectively. b, Receptor binding profile of RG-EA2HA1-N121T, HA1-Y138H, HA1-N207Y, HA1-K311Q, HA2-A65S, and HA2-D158N. Glycan array data (left panel) are shown with the mean and SD fluorescence (RFU) calculated from 6 replicate spots of each glycan (left panel), and the enzyme-linked immunosorbent assay (right panel) results are shown with the mean and SD absorbance (450 nm) from 3 replicates in one of two independently performed experiment. c, The contact transmissibility of RG-EA2xEA3SG virus containing the internal genes from RG-EA2 and the surface genes derived from RG-EA3

in pigs. Contact transmission experiments were performed in duplicate with a total of four donors and four direct contacts. Pigs housed in the same pen are denoted by the same colour. The limit of detection (1.789 log10TCID50/mL) is shown with the horizontal dashed line.

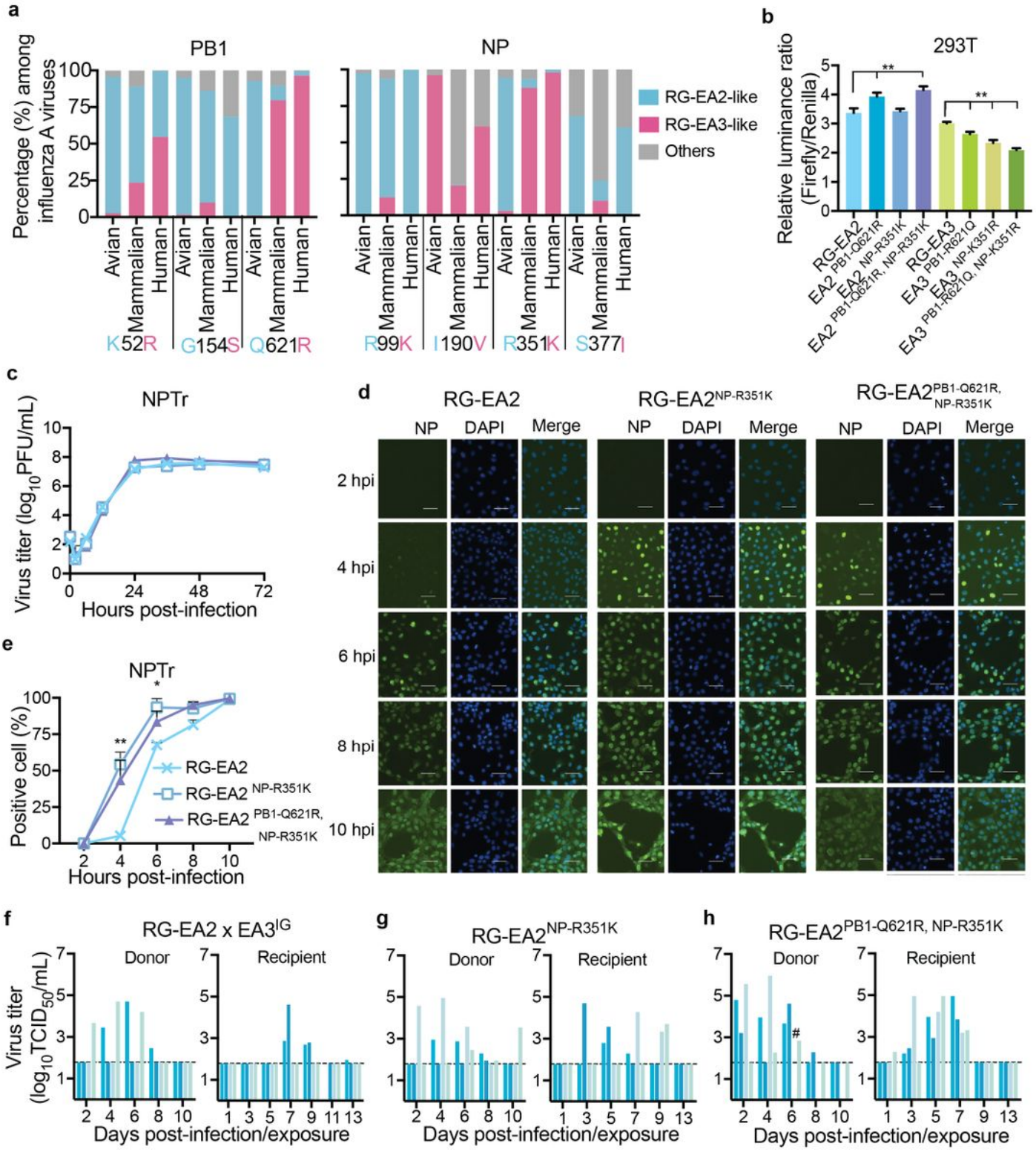


Figure 5

The NP-R351K mutation that has been under strong positive selection among EA swine influenza viruses was the minimal molecular change required to facilitate transmission of the non-transmissible RG-EA2

virus. a, Detection frequency of Q/R at PB1 residue 621 (N = 74,095) and R/K at NP residue 351 (N = 80,188) among mammalian and human influenza A viruses. b, The effects of amino acid substitutions at PB1 residue 621 and NP residue 351 on viral polymerase activity were determined using minigenome assay in 293T cells. The mean and SD ratio of firefly/ renilla luciferase from three repeats in one of two independently performed experiment is shown. One-way ANOVA with Tukey's multiple comparison test was performed (**P < 0.01). (c) Multicycle replication kinetics of recombinant viruses in NPTr cells. Mean and SD from three repeats in one experiment is shown. d,e, Nucleus localization of NP protein in NPTr cells infected with RG-EA2, RG-EA2NP-R351K, and RG-EA2PB1-Q621R, NP-R351R at MOI of 5 at different time points. Representative images from three replicates of one experiment are shown (Scale bar: 100 μM) (d). Mean and SD of NP positive rate (NP positive cells per DAPI positive cells, %) from three replicated of one experiment are calculated at different hours post-infection (e). Two-way ANOVA with Tukey's multiple comparisons post hoc test were performed (*P < 0.05 and **P <0.01). f,g,h, The contact transmissibility of RG-EA2xEA3IG virus (f), RG-EA2 NP-R351K (g), and RG-EA2 PB 1-Q621R,NP-R351K in pigs. Contact transmission experiments were performed in duplicate with a total of four donors and four direct contacts. Pigs housed in the same pen are denoted by the same colour. The limit of detection (1.789 log10TCID50/mL) is shown with the horizontal dashed line. # indicates a donor in the RG-EA2 PB 1-Q621R,NP-R351K group euthanized on day 4 post-infection due to respiratory distress with abdominal distention, severe lethargy, and vomiting.

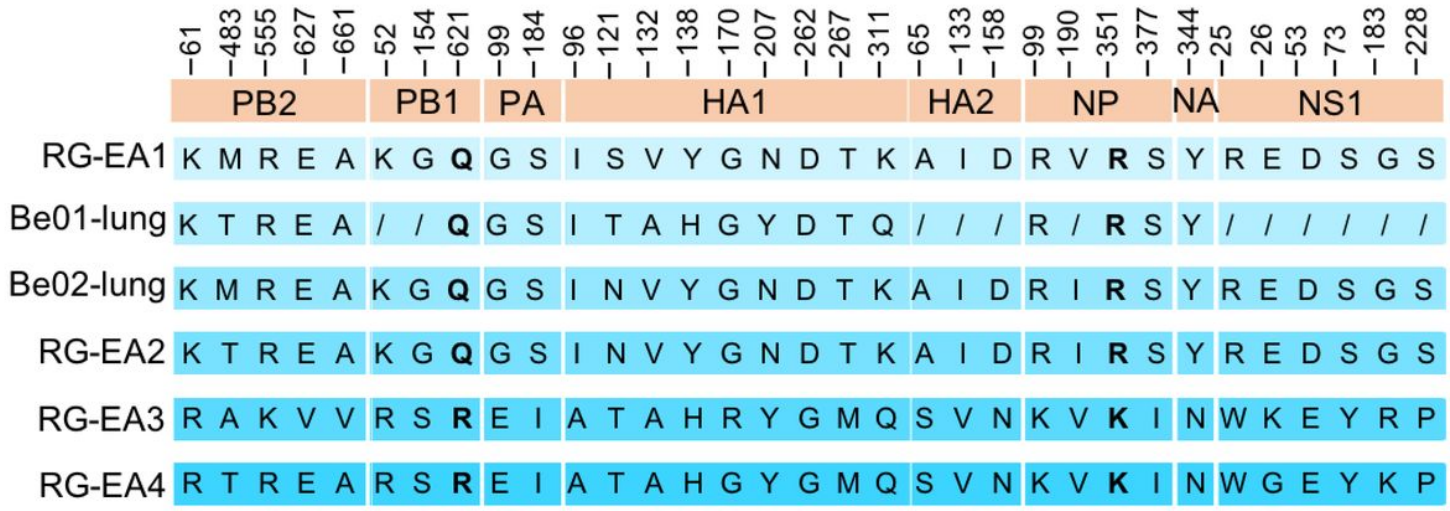


Figure 6

Direct sequencing of EA swine viruses from archived pig lung homogenates in 1979 validated the robustness of ancestral sequence reconstruction in resurrecting recombinant viruses that represented different evolutionary stages. Full genome of A/swine/Belgium/2/1979 (Be02-lung) and a partial genome of A/swine/Belgium/1/1979 (Be01-lung) EA swine influenza viruses were sequenced from two archived pig lung homogenates from 1979. Four recombinant viruses were resurrected using ancestral sequence reconstruction, with RG-EA1 representing the precursor virus of EA swine viruses, RG-EA2 representing the early evolutionary stage of EA swine viruses in 1979-1983, and RG-EA3 and RG-EA4 representing EA

swine viruses in 1984-1987 and 1988-1992, respectively. Among the 33 amino acids that differentiate the non-transmissible RG-EA2 virus and transmissible RG-EA3 virus, the sequences of Be01 and Be02 showed high homology to RG-EA2. /, unsuccessfully determined.

Supplementary Files

This is a list of supplementary files associated with this preprint. Click to download.

- Supplementaryinformationv11.pdf